29 April 1994

ELSEVIER

Chemical Physics Letters 221 (1994) 453–458

CHEMICAL PHYSICS LETTERS

How free are encapsulated atoms in C_{60}?

Y.S. Li [a], D. Tománek [b]

[a] *Biosym Technologies, Inc., 9685 Scranton Road, San Diego, CA 92121, USA*
[b] *Department of Physics and Astronomy, Michigan State University, East Lansing, MI 48824-1116, USA and Center for Fundamental Materials Research, Michigan State University, East Lansing, MI 48824-1116, USA*

Received 25 January 1994

Abstract

We calculate the interaction between encapsulated Li, K and O atoms and the C_{60} cage in $M@C_{60}$ endohedral complexes from first principles. The $M–C_{60}$ bond is purely ionic for K, and has only a small covalent contribution for Li. The K and Li atoms are confined within the nearly sperical potential well, and exhibit low-frequency rolling and high-frequency rattling vibrational modes. Oxygen prefers to bind on a C–C bridge site by a strongly covalent epoxy bond which locally modifies the cage and leads to a large anisotropy in the $O–C_{60}$ interaction potential.

The discovery [1] and mass production [2] of the C_{60} molecule ignited a strong interest in carbon fullerenes and fullerene-derived structures. An important motivation for chemical modification was the discovery of superconductivity in donor-element intercalated C_{60} solids [3]. The next logical step following the formation of such exohedral compounds was to encapsulate atoms in the fullerene cage, leading to molecular endohedral complexes. These systems would provide a unique possibility to tailor specific materials properties, such as dielectric response, optical spectra, and reactivity, on a molecular level [4–10]. A potentially important application of these internally doped molecules is the possibility of their assembly to a bulk superconductor with a potentially very different value of the critical temperature T_c than found in the extrinsically intercalated C_{60} crystal [3,11].

The successful synthesis of $M@C_{60}$ complexes in the gas phase [4] calls for a reliable calculation of their properties. The equilibrium geometry and the stability of several systems have been computed using both ab initio and semi-empirical electronic structure calculations [5–10]. These calculations suggest that, similar to exohedral C_{60} intercalation compounds, the most stable systems involve donor atoms, especially from the alkali, alkaline earth and rare earth series. The $M@C_{60}$ systems are stabilized primarily by the large Coulomb interaction, originating in the charge transfer between the enclosed atoms and the C_{60} cage. Extra stabilization is gained when the enclosed ion moves off-center, causing a polarization of the shell.

This unusual intramolecular $M–C_{60}$ interaction, together with the fact that the size of the enclosed atom is much smaller than the cage, is expected to yield an interesting vibration spectrum of the system. A particularly interesting problem is the degree of freedom of the encapsulated atoms in the C_{60} cage. In this Letter, we report the results of the first molecular dynamics simulation for the $M@C_{60}$ system at different temperatures. We show that differences in the bonding characteristics between different $M@C_{60}$ systems lead to significantly different low-frequency

SSDI 0009-2614(94)00297-4

angular motion ('rolling') and radial vibration ('rattling') modes of the enclosed atom. We focus on three systems: Li@C_{60}, K@C_{60}, and O@C_{60}. The first two systems are model donor complexes with a different degree of ionicity, the third is an acceptor system. Our objective is first to determine the equilibrium geometry of the endohedral complexes and the potential energy surface describing the M–C_{60} interaction. A challenging part of this calculation is to address correctly the changing degree of covalency for different positions of M inside C_{60}. This information is subsequently used to calculate the dynamics of the system.

The calculation is performed using the DMol cluster code [12], an implementation of the density functional theory within the local density approximation (LDA) [13]. The molecular orbitals are represented by linear combinations of numerically generated basis functions. In the double-numerical basis set [12], the C2s and C2p orbitals are represented by two wavefunctions each, and a 3d type wavefunction on each carbon atom is used to describe polarization. Consequently, the C_{60} basis consists of 780 orbitals. We use the frozen core approximation to treat the inner core electrons and the von Barth and Hedin potential to describe the exchange–correlation energy [14]. We determine the M–C_{60} interaction in the following two steps. First, we freeze the C_{60} cage and calculate the total energy while displacing the enclosed atom along several high-symmetry directions, starting at the center of the cage. For each geometry, our calculations also yield the electronic structure and M–C_{60} bond characteristics. Next, we determine the equilibrium geometry and total energy of M@C_{60} using an unrestricted optimization of this system, starting from the energy minima in the above potential energy surface. This is achieved by moving all atoms in the direction of analytically calculated forces, until all forces are smaller than 0.05 eV/Å. We calibrate the accuracy of this procedure on the free C_{60} molecule. We find for the cohesive energy of C_{60} the value 8.364 eV/atom, and for the gap between the highest occupied and lowest unoccupied molecular orbitals (HOMO–LUMO gap) 1.64 eV. The bond lengths are determined to be 1.39 and 1.44 Å for double and single bonds [#1], respectively. These values agree well with early LDA results [15] and NMR and gas-phase electron diffraction data [16,17].

In Fig. 1, we plot the M–C_{60} binding energy in M@C_{60} for Li, K, and O as a function of the off-center distance of the enclosed atom, along different symmetry directions. Our results indicate that all three complexes are stable with respect to the free C_{60} and the isolated atoms, with the binding energy $E_b = -1.89$ eV for Li@C_{60}, -2.25 eV for K@C_{60}, but only -0.06 eV for O@C_{60}. This predicted lowest stability of endohedral *acceptor* complexes is in agreement with previous estimates [10], and can be understood from a detailed electronic structure analysis given below.

The Li–C_{60} binding energy, shown in Fig. 1a, has a very similar shape along all symmetry directions considered, with energy minima occurring at 1.5 Å off-center. The well depths are about 0.7 eV along the different high-symmetry directions investigated. The

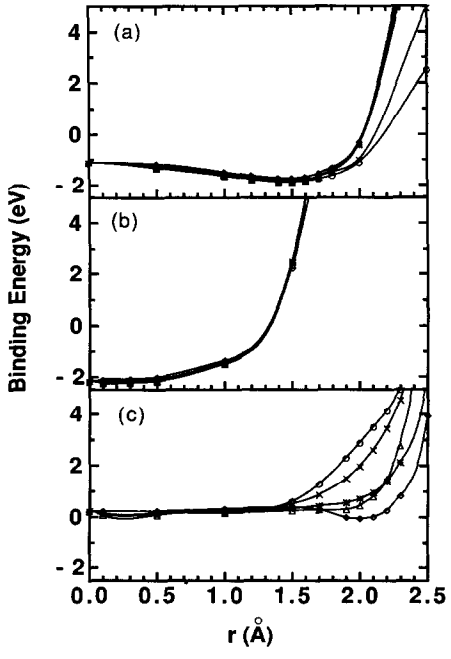

Fig. 1. Calculated M–C_{60} binding energy E_b in M@C_{60} endohedral complexes, as a function of the off-center distance r of the enclosed atom. The results are given for (a) Li, (b) K, and (c) O based complexes. The high-symmetry displacement directions connect the center of C_{60} and the C atoms of the cage (△), the centers of the C–C single bonds (*) and double bonds (◇), the centers of the hexagons (○), and the centers of the pentagons (×).

[#1] We call C–C bonds shared by a pentagon and a hexagon 'single' bonds, and all other bonds 'double' bonds.

Li–C_{60} interaction in Li@C_{60} is predominantly ionic, with only a small covalent contribution involving the Li2s electron. This is reflected in a near-uniform shift of the LDA level spectrum of Li@C_{60} with respect to the C_{60} molecule. The ionic bond character results in a nearly isotropic potential energy surface with an approximate shape of a hollow spherical shell. The barriers between potential energy minima are relatively small. Consequently, the enclosed Li atom moves rather freely near a spherical surface inside the cage, at a distance of ≈ 1.5 Å from the origin. The moderate anisotropy of this potential energy surface results from a covalent contribution to the bond strength near the potential minima. The degree of hybridization can be qualitatively investigated using the Mulliken population analysis. Our results indicate that the charge transferred from Li to the C_{60} shell decreases from 0.8 to 0.3 electrons as Li is moved from the center of C_{60} to the equilibrium off-center distance. This decreasing charge transfer reflects an increasing hybridization between Li and C_{60} and an increasing bond covalency. The transferred charge originates mainly from the Li2s states, and is transferred to the t_{1u} LUMO of C_{60}. The dipole moment of Li@C_{60} in the equilibrium geometry has the huge value of 15.7 D [#2].

The cage center is a local maximum of the potential energy surface. The 0.7 eV off-center stabilization energy results from the polarization of the cage, as suggested earlier [5–10]. The upper limit of this polarization energy can be estimated using a classical model of a point charge in a thin metal shell [#3], as $E_{pol} = -q^2d^2/R(R^2-d^2)$. Here, $R = 3.53$ Å is the radius of the C_{60} molecule, d is the off-center distance and q is the net charge of the Li cation. This simple model yields $E_{pol} = 0.7$ eV in agreement with our ab initio results, if we use the value $q = 0.58\ e$ near the potential minimum, given by the Mulliken analysis.

Compared with the Li@C_{60} complex, the potential energy surface of K@C_{60}, shown in Fig. 1b, is rather simple and isotropic. It is very flat in the region close to the cage center, with a minimum of -2.25 eV at a small off-center distance of ≈ 0.25 Å. The stronger radial confinement of K (as compared to Li) results from a larger M–C_{60} repulsion for this heavier ion. This is due to the large ionic radius of K, $r_{ion} = 1.3$ Å, in comparison to $r_{ion} = 0.7$ Å for Li. The Mulliken analysis indicates that the K atom loses its 4s valence electron completely to the C_{60} cage. We also find that the net charge of K does not change between the cage center and the equilibrium off-center sites. The purely ionic K–C_{60} interaction results in an isotropic potential. As we discuss later on, the flat potential energy surface close to the cage center gives rise to very low-frequency rolling and rattling modes of K in the C_{60} cage. The ionic character of the K–C_{60} bond is also reflected in a rigid shift of the LDA level spectrum of K@C_{60} with respect to the C_{60} molecule. The equilibrium off-center position of K in C_{60} yields a large dipole moment for K@C_{60} amounting to 8.8 D.

The ionization potential of C_{60}, $I(C_{60}) = 7.54$ eV, is much larger than the electron affinity value $A(C_{60}) = 2.74$ eV [18], which makes C_{60} a much better electron acceptor than electron donor. Consequently, we expect an ionic endohedral complex O@C_{60} with divalent oxygen to be energetically unstable. The Mulliken charge of the O atom is indeed relatively small, $q \approx -0.4\ e$, and does not change much with changing absorption geometry. Our energy results for this system, shown in Fig. 1c, indicate that the O@C_{60} complex is only stable in a geometry where oxygen bridges a C–C double bond. This fact, together with the small Mulliken charge on the oxygen atom, is indicative of a strongly covalent O–C_{60} bond character.

As mentioned above, we performed an unrestricted geometry optimization including shell relaxation for all the systems considered. We expect only a negligible cage relaxation due to up to one delocalized transferred electron in the Li@C_{60} and K@C_{60} systems which are stabilized by an ionic interaction. Indeed, our results indicate an increase of the C–C bond lengths by an amount less than 0.01 Å and a total energy decrease by < 0.1 eV for both Li@C_{60} and K@C_{60} complexes. Therefore, we believe that the potential energy surface calculated above represents well the real M–C_{60} interaction in these two systems and can be used to determine the detailed motion of encapsulated Li and K atoms.

Unlike in the donor complexes, we expect significant C_{60} cage deformations in O@C_{60}, resulting from the strongly covalent O–C_{60} interaction. We opti-

[#2] 1 D is the dipole moment of an e^+e^- pair separated by 0.208 Å.

[#3] Of course, the metal shell model *cannot* describe the static dipole moment of the system.

mized the geometry of $O@C_{60}$ starting from an initial position of the O atom 2.0 Å off-center, in the direction towards the center of the C–C double bond. Our results indicate a strong covalent interaction between the oxygen atom and this C–C bond, which stabilizes the $O@C_{60}$ system by 1.58 eV. At the same time, this strong 'inside epoxy' bond weakens significantly the C–C double bond bridged by the oxygen atom, resulting in its elongation from 1.39 to 1.43 Å. As a consequence, the length of the other bonds in the two adjacent carbon hexagons increases by 0.01–0.05 Å. The equilibrium separation of the oxygen atom from the cage center is ≈ 1.84 Å, and from the nearest neighbor C atoms 1.50 Å. The strong and localized O–C_{60} bond causes a large anisotropy in the interaction potential between oxygen and the C_{60} cage. Therefore, we do not expect any significant 'rattling' or 'rolling' motion of oxygen inside the cage.

In order to determine the detailed motion of encapsulated Li and K atoms in C_{60}, we have performed a molecular dynamics calculation. The most convenient way to determine the forces acting on the trapped atom is to use a model potential $V(r)$ which fits accurately our above results for the M–C_{60} interaction at high-symmetry sites. We found that this can be achieved by combining the C_{60} polarization energy and a pairwise M–C repulsive interaction, which can be parametrized as

$$V(r) = V_0 - \frac{(ar^2+b)e^2}{R(R^2-r^2)}r^2 + \epsilon_0 \sum_{i=1}^{60} \{\exp[-\beta(|r-r_i|-r_0)] - \exp[-\beta(R-r_0)]\} + \epsilon_1 r(r+c) \sum_{i=1}^{60} \exp[-\gamma(1-\hat{r}\cdot\hat{r}_i)^2] . \quad (1)$$

This potential form addresses the essential physics of the Li–C_{60} and K–C_{60} interaction which is predominantly ionic. Since this potential cannot describe covalent interactions, we do not use it for the $O@C_{60}$ potential energy surface. In contrast to a potential previously suggested by Schmidt et al. [19], we describe the polarization energy of the system using a metallic shell model for C_{60} rather than considering the individual atoms (see footnote 3). In Eq. (1), r is the position of the enclosed atom, and r_i are the positions of the C_{60} cage atoms in a coordinate system anchored at the center of C_{60}. V_0 is the potential at the cage center, and R is the radius of the C_{60} cage. a, b, ϵ_0, β, and r_0 are parameters. The expression $(ar^2+b)e^2$ in the second term is used to parametrize the net charge on the enclosed atom as a function of its off-center distance r. The third and fourth term address the non-Coulombic and anisotropic parts of the interaction between the enclosed atom and the C_{60} cage. The numerical values of these parameters, which reproduce our LDA results for the endohedral complexes, are the following. For $Li@C_{60}$, we find $V_0 = -1.123$ eV, $a = -10.21$ Å^{-2}, $b = 59.65$, $\epsilon_0 = 0.0654$ eV, $\beta = 1.225$ Å^{-1}, $r_0 = 3.780$ Å, $\epsilon_1 = -5.77 \times 10^{-4}$ eV Å^{-2}, $c = 141.9$ Å, and $\gamma = 5.18 \times 10^4$. For $K@C_{60}$, we use $V_0 = -2.182$ eV, $a = -37.425$ Å^{-2}, $b = 21.341$, $\epsilon_0 = 0.261$ eV, $\beta = 1.734$ Å^{-1}, $r_0 = 1.711$ Å, and $\epsilon_1 = 0$. The larger value of β and r_0 for $K@C_{60}$ reflects the stronger K–C_{60} repulsion. The minimum energy and the $V=0$ potential energy surfaces for $Li@C_{60}$ are given in Fig. 2. These results reflect the large degree of covalency in the Li–C_{60} bond, causing a large potential anisotropy, and the spatial confinement of Li in C_{60}. The analogous $K@C_{60}$ potential surfaces are nearly isotropic and show a much larger degree of confinement of K inside C_{60}.

In order to determine the degree of spatial freedom of the encapsulated atoms, we performed a series of molecular dynamics calculations for Li and K in C_{60} at various temperatures. In particular, we investigated the vibrational modes of the enclosed atoms by analyzing the power spectra of their time-dependent trajectories. For each system and temperature, we used Nosé–Hoover molecular dynamics to calculate 30 trajectories starting at different points. In each simulation, we followed the trajectory of the encapsulated atom for 1.75×10^6 time steps of 0.2×10^{-15} s, thus probing efficiently the phase space.

The vibrational spectra of the enclosed atom in $Li@C_{60}$ and $K@C_{60}$, shown in Fig. 3, are characterized by a low-frequency and a high-frequency peak. In order to characterize these modes, we decomposed the atomic trajectories into radial and an angular components. Inspection of the radial spectra, shown in the insets of Figs. 3a and 3b, suggests that the high-frequency modes at 370 cm^{-1} for Li and 86 cm^{-1} for K are the radial 'rattling' modes. A very similar value

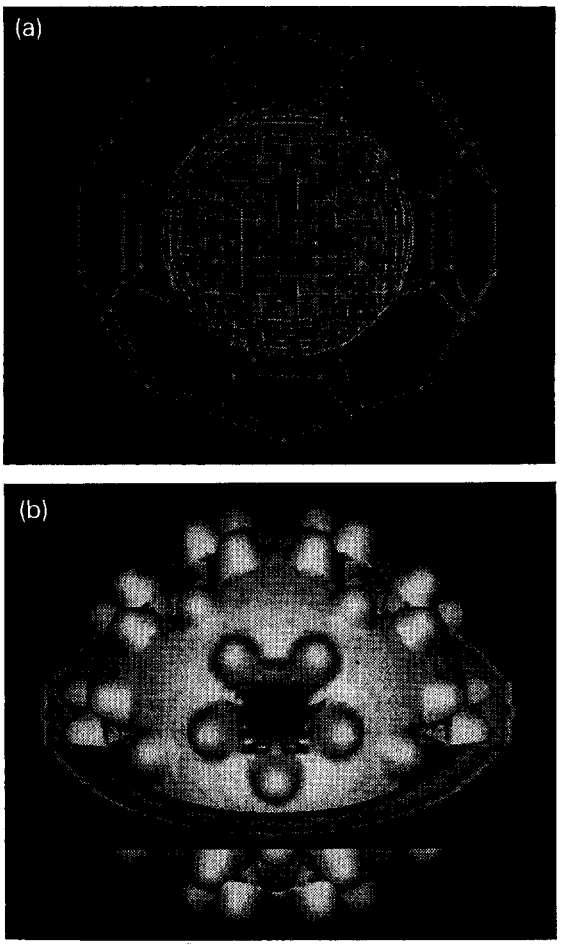

Fig. 2. Three-dimensional view of the Li–C_{60} potential energy $V(r)$ for Li@C_{60}. (a) The $V=0$ surface (mesh) and the enclosed $V=V_{min}+0.10$ eV surface, which is close to the minimum-energy surface. The position of the C_{60} cage is shown schematically to scale. (b) Detailed view of the $V=V_{min}+0.12$ eV energy surface.

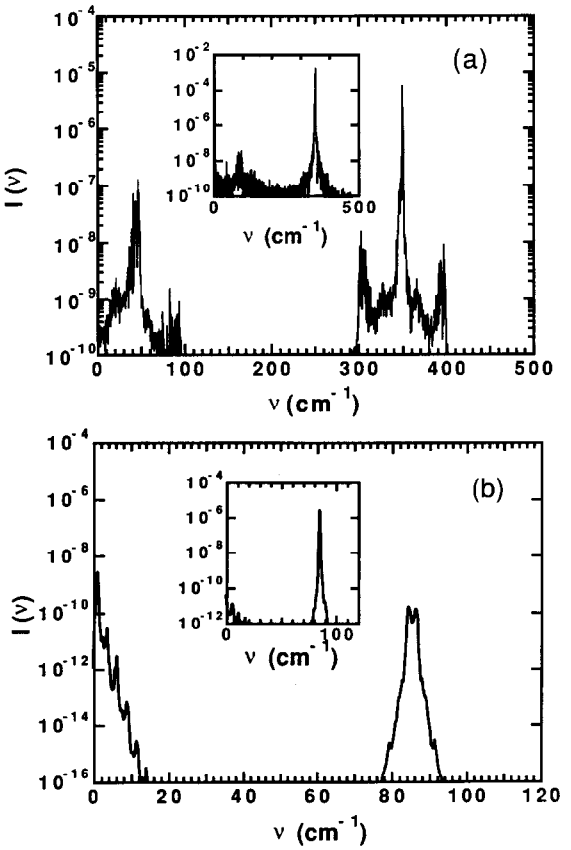

Fig. 3. Vibrational spectra $I(\nu)$ of (a) Li in Li@C_{60} and (b) K in K@C_{60} at $T=50$ K, obtained from molecular dynamics simulations. The radial 'rattling' modes, obtained from a radial projection of the atomic trajectories and shown in the insets of (a) and (b), correspond to the high-frequency modes at 370 and 86 cm^{-1} for Li and K, respectively. The low-frequency peaks in the vibrational spectra correspond to the 'rolling' modes of the encapsulated atoms.

of 340 cm^{-1} for the 'rattling' modes in Li@C_{60} has been obtained previously by Dunlap [6]. Our calculated value of the 'rattling' frequency of the heavier K lies in the same range as the published value for Na@C_{60} [19].

The low-frequency peaks in the vibrational spectra at 40–50 cm^{-1} for Li@C_{60} and <10 cm^{-1} for K@C_{60} correspond to the 'rolling' modes of the encapsulated atoms around the cage center. Due to the moderate anisotropy of the Li–C_{60} potential, initiation of the Li 'rolling' motion is a thermally activated process. From the inspection of Li trajectories at different temperatures, we conclude that these 'rolling' modes get activated above a critical temperature of ≈ 40 K. This value agrees reasonably well with an energy barrier of ≈ 0.002 eV, estimated from our LDA results. The particular anisotropy found in the Li–C_{60} potential introduces a strong coupling between the angular 'rolling' and the radial 'rattling' modes. This coupling broadens both the low-frequency 'rolling' and the high-frequency 'rattling' modes with increasing temperature. The unexpectedly low value of the K 'rattling' and 'rolling' modes in K@C_{60} is caused partly by the larger mass of K, and partly by the flatness and near-isotropy of the K–C_{60} potential near the cage center. Due to the non-vanishing dipole mo-

ments of the endohedral complexes, these modes should be observable in infrared spectra.

The authors appreciate useful discussions with Dr. Ciao Lewenkopf. YSL acknowledges financial support by the US Department of Energy and Sandia National Laboratories under contract No. DE-AC04-76DP00789, and the Condensed Matter Theory group at Michigan State University. DT appreciates support by the National Science Foundation under Grant No. PHY-8920927 and the Air Force Office of Scientific Research under Grant No. F49620-92-J-0523DEF. Computer time has been provided by a grant from the National Supercomputing Center for Energy and the Environment at the University of Nevada in Las Vegas.

References

[1] H.W. Kroto, J.R. Heath, S.C. O'Brien, R.F. Curl and R.E. Smalley, Nature 318 (1985) 162.

[2] W. Krätschmer, L.D. Lamb, K. Fostiropoulos and D.R. Huffman, Nature 347 (1990) 354.

[3] A.F. Hebard, M.J. Rosseinsky, R.C. Haddon, D.W. Murphy, S.H. Glarum, T.T.M. Palstra, A.P. Ramirez and A.R. Kortan, Nature 350 (1991) 600;
M.J. Rosseinsky, A.P. Ramirez, S.H. Glarum, D.W. Murphy, R.C. Haddon, A.F. Hebard, T.T.M. Palstra, A.R. Kortan, S.M. Zahurak and A.V. Makhija, Phys. Rev. Letters 66 (1991) 2830.

[4] Y. Chai, T. Guo, C. Jin, R.E. Haufler, L.P.F. Chibante, J. Fure, L. Wang, J.M. Alford and R.E. Smalley, J. Phys. Chem. 95 (1991) 7564;
M.M. Alvarez, E.G. Gillan, K. Holczer, R.B. Kaner, K.S. Min and R.L. Whetten, J. Phys. Chem. 95 (1991) 10561.

[5] J. Cioslowski and E.D. Fleischmann, J. Chem. Phys. 94 (1991) 3730;
J. Cioslowski and A. Nanayakkara, Phys. Rev. Letters 69 (1992) 2871.

[6] B.I. Dunlap, J.L. Ballester and P.P. Schmidt, J. Phys. Chem. 96 (1992) 9781.

[7] B. Wästberg and A. Rosén, Physica Scripta 44 (1991) 276.

[8] S.C. Erwin, in: Buckminsterfullerenes, eds. W.E. Billups and M.A. Ciufolini (VCH Publishers, Weinheim, 1993) pp. 217–255.

[9] H. Schwarz, T. Weiske, D.K. Böhme and J. Hrušák, in: Buckminsterfullerenes, eds. W.E. Billups and M.A. Ciufolini (VCH Publishers, Weinheim, 1993) pp. 257–283.

[10] Y. Wang, D. Tománek and R.S. Ruoff, Chem. Phys. Letters 208 (1993) 79.

[11] M. Schluter, M. Lannoo, M. Needels, G.A. Baraff and D. Tománek, Phys. Rev. Letters 68 (1992) 526.

[12] B. Delley, J. Chem. Phys. 92 (1990) 508.

[13] P. Hohenberg and W. Kohn, Phys. Rev. B 136 (1964) 864; W. Kohn and L.J. Sham, Phys. Rev. A 140 (1965) 1133.

[14] U. von Barth and L.J. Hedin, J. Phys. C 5 (1972) 1629.

[15] B.I. Dunlap, Intern. J. Quantum Chem. Symp. 22 (1988) 257.

[16] C.S. Yannoni, P.P. Bernier, D.S. Bethune, G. Meijer and J.R. Salem, J. Am. Chem. Soc. 113 (1991) 3190.

[17] K. Hedberg, L. Hedberg, D.S. Bethune, C.A. Brown, H.C. Dorn, R.D. Johnson and M. Devries, Science 254 (1991) 410.

[18] I.V. Hertel, H. Steger, J. de Vries, B. Weisser, C. Menzel, B. Kamke and W. Kamke, Phys. Rev. Letters 68 (1992) 784; S.H. Yang, C.L. Pettiette, J. Conceicao, O. Chesnovsky and R.E. Smalley, Chem. Phys. Letters 139 (1987) 233.

[19] P.P. Schmidt, B.I. Dunlap and C.T. White, J. Phys. Chem. 95 (1991) 10537.